

Long-time tails of the velocity autocorrelation function in two- and three-dimensional lattice-gas cellular automata: A test of mode-coupling theory

M. A. van der Hoef and D. Frenkel

FOM-Institute for Atomic and Molecular Physics, P.O. Box 41883, 1009 DB Amsterdam, The Netherlands

(Received 11 September 1989)

We report simulations of the velocity autocorrelation function (VACF) of a tagged particle in two- and three-dimensional lattice-gas cellular automata, using a new technique that is about a million times more efficient than the conventional techniques. The simulations clearly show the algebraic $t^{-D/2}$ tail of the VACF. We compare the observed long-time tail with the predictions of mode-coupling theory. In three dimensions, the amplitude of this tail is found to agree within the (small) statistical error with these predictions. In two dimensions small but significant deviations from mode-coupling theory of up to 5% are observed.

I. INTRODUCTION

The velocity autocorrelation function (VACF) is a function of fundamental interest in atomic fluids. Until 1970 it was generally believed to decay exponentially for long times; however, in 1970 Alder and Wainwright¹ found by molecular-dynamics simulation that the asymptotic decay of the VACF is slower than the exponential decay. Their findings indicated that for times much longer than the mean free time t_0 , the VACF decays algebraically with an exponent $D/2$, where D is the dimensionality. The Alder-Wainwright results caused a complete overhaul of the kinetic theory of dense fluids. The subsequent theoretical analyses of algebraic long-time tails were either based on an extension of kinetic theory² or on mode-coupling theory.³ For a review, see Ref. 4. In the mode-coupling theory by Ernst, Hauge, and van Leeuwen,³ it is assumed that the long-time tail is the consequence of coupling between particle diffusion and shear modes in the fluid. More recent simulations of hard-core fluids in both two and three dimensions confirmed the existence of the algebraic tail.^{5,6} The most recent simulation for a three-dimensional (3D) atomic system is by Erpenbeck and Wood.⁷ These authors observed agreement between their simulation results of the VACF and a finite- N mode-coupling theory for some densities. Nevertheless, the statistical accuracy of their data was such that it was not meaningful to verify either the value of the exponent of the algebraic tail or the functional form of the density-dependent tail coefficient independently.

Lattice-gas models have recently been revived as an alternative for simulating atomic fluids.⁸ Because of their simple structure, which makes it comparatively easy to work out the consequences of a particular approximation scheme, they are ideally suited to serve as a testing ground for concepts in kinetic theory. Hence lattice-gas models seem to be an attractive alternative for determining the VACF. This approach has been tried by Boon and Noullez⁹ and Binder and d'Humières¹⁰ for 2D systems. However, due to poor statistics, long-time tails could not be detected.

In this paper we first discuss lattice-gas models in general. In Sec. III we present a mode-coupling theory for lattice-gas models. In Sec. IV we present a computational scheme that makes it possible to compute the VACF of lattice gases with hitherto unachievable accuracy. In Sec. V we present the simulation results using this new method and compare it with the lattice-gas version of mode-coupling theory.

II. LGCA MODELS

Let us first briefly summarize the essentials of lattice-gas cellular automata (LGCA), in order to establish the notation that is used in subsequent sections. In what follows, we assume that the reader is familiar with the basics of lattice-gas models. For more details on this subject the reader is referred to, for instance, Refs. 8, 11, 12, and 13.

In LGCA models, time and space are considered discrete. This means that the model system is defined on a lattice and the state of the automation is only defined at regular points in time with separation Δt . At every time step particles are only allowed to be situated at lattice nodes, with possible velocities \mathbf{c}_i , $i \in \{1, 2, \dots, b\}$. The set \mathbf{c}_i can be chosen in many different ways, although they are restricted by the constraint that

$$\mathbf{r}' + \mathbf{c}_i \Delta t = \mathbf{r}'',$$

where \mathbf{r}' and \mathbf{r}'' are neighboring lattice nodes. In the present paper the velocity set of the three-dimensional model is defined by the additional constraint that $|\mathbf{c}_i| = c$, whereas in the two-dimensional model the set is defined by $|\mathbf{c}_1| = 0$ and $|\mathbf{c}_i| = c$ for $i \neq 1$. We can imagine a particle at node \mathbf{r} with velocity \mathbf{c}_i as occupying a link connecting the node \mathbf{r} with the nearest-neighbor node $\mathbf{r} + \mathbf{c}_i \Delta t$. No two particles can be at the same lattice node with the same velocity. The time evolution of the LGCA consists of two steps:

(1) *Propagation.* All particles move in one time step Δt from their initial lattice position \mathbf{r} to a new position $\mathbf{r}' = \mathbf{r} + \mathbf{c}_i \Delta t$. For convenience we choose $\Delta t = 1$.

(2) *Collision.* The particles at all lattice nodes undergo a collision that conserves the total number of particles and the total momentum at each node. The collision rules may or may not be deterministic.

The state of the automaton at time (point) t is completely given by $s_i(\mathbf{r}, t)$, which is equal to 1(0) if a particle is present (absent) on node \mathbf{r} with velocity c_i .

Provided the lattice has sufficiently high symmetry, the equation that governs the time evolution of the distribution function of such a lattice gas becomes equivalent to the Navier-Stokes equation for an incompressible fluid if the flow velocity is much less than the speed of sound, and all spatial variations in the system occur on a scale that is large compared to the mean free path of the lattice-gas particles. In this respect LGCA's model atomic fluids.

The models under consideration are the two-dimensional Frisch-Hasslacher-Pomeau model with seven possible velocities on a triangular lattice (generally denoted as the FHP-III model), and the three-dimensional face-centered hypercubic (FCHC) model.^{11,13} The FHP-III is discussed extensively elsewhere,^{11,12} but the 3D FCHC model that we use will need some comment. In this lattice there are 24 possible velocities, so a collision would require a 2^{24} -word lookup table, which requires a very large shared memory.¹⁴ In the algorithm used in the present paper the 24-bit state is split into two 12-bit sub-states,¹⁵ which requires only a small 12-bit lookup table. This splitting can be done in six different way, one of which is chosen randomly at every collision. The parameter Re_*^{\max} measuring the effectiveness of the collision rules is about two, similar to Hénon's isometric rules.¹⁶ Much higher values for Re_*^{\max} can be achieved.^{14,17} However, for the present simulation a high value of Re_*^{\max} is not necessary; hence we employ the simple 12-bit rules. An explicit expression for the kinematic viscosity and the diffusion coefficient that follows from the Boltzmann-Enskog equation for this 3D model is given in Appendix A.

III. MODE-COUPLING THEORY FOR LGCA

The extension of mode-coupling theory to lattice gases was first presented by Kadanoff *et al.*¹⁸ Here the more intuitive derivation by Ernst¹⁹ is given, which is based on the Ernst-Hauge-van Leeuwen (EHVL) theory for continuous systems.³ In addition to $s_i(\mathbf{r}, t)$, we define $n_i(\mathbf{r}, t)$ which is the occupation number of a tagged particle. The VACF is then given by

$$\langle v_x(0)v_x(t) \rangle = \sum_{\mathbf{r}_0} \sum_{i_0} \sum_{\mathbf{r}} \sum_i c_{i_0x} c_{ix} \langle n_{i_0}(\mathbf{r}_0, 0)n_i(\mathbf{r}, t) \rangle. \quad (1)$$

Note that the initial value is equal to

$$\langle v_x^2(0) \rangle = \frac{1}{bV} \sum_{\mathbf{r}} \sum_i c_{ix}^2, \quad (2)$$

where V is the number of lattice nodes. Some average values that will be useful are

$$\begin{aligned} \langle s_i(\mathbf{r}, t) \rangle &= \frac{\rho}{b}, \\ \langle n_i(\mathbf{r}, t) \rangle &= \frac{1}{bV}, \\ \langle n_{i_0}(\mathbf{r}_0, 0)n_i(\mathbf{r}, 0) \rangle &= \delta_{i_0i} \delta_{\mathbf{r}_0\mathbf{r}} \frac{1}{bV} + O\left[\frac{1}{V^2}\right], \\ \langle n_{i_0}(\mathbf{r}_0, 0)s_i(\mathbf{r}, 0) \rangle &= \frac{\rho}{b^2V} + \delta_{i_0i} \delta_{\mathbf{r}_0\mathbf{r}} \frac{1}{bV} \left[1 - \frac{\rho}{b}\right], \end{aligned} \quad (3)$$

where ρ is the average number of particles per site. Following EHVL, we now introduce the special nonequilibrium (NE) ensemble average $\langle \rangle_{\text{NE}}$, which is equal to the equilibrium ensemble under the constraint that at $t=0$ the phase coordinates of the tagged particle are (\mathbf{r}_0, i_0) and is written in terms of the equilibrium ensemble average as

$$\langle A_i(\mathbf{r}, t) \rangle_{\text{NE}} = \frac{\langle n_{i_0}(\mathbf{r}_0, 0)A_i(\mathbf{r}, t) \rangle}{\langle n_{i_0}(\mathbf{r}_0, 0) \rangle}, \quad (4)$$

where $A_i(\mathbf{r}, t)$ can be any dynamical variable. Then the VACF can be written as

$$\begin{aligned} \langle v_x(0)v_x(t) \rangle &= \frac{1}{bV} \sum_{\mathbf{r}_0} \sum_{i_0} \sum_{\mathbf{r}} \sum_i c_{i_0x} c_{ix} \langle n_i(\mathbf{r}, t) \rangle_{\text{NE}} \\ &= \frac{1}{bV} \sum_{\mathbf{r}_0} \sum_{i_0} \sum_{\mathbf{r}} \sum_i c_{i_0x} c_{ix} f_i^{\text{NE}}(\mathbf{r}, t), \end{aligned} \quad (5)$$

where $f_i^{\text{NE}}(\mathbf{r}, t)$ the NE distribution function of a tagged particle. In the spirit of the EHVL method we coarse grain over cells, containing many sites, and replace the lattice sum over sites by a lattice sum over cells. We now use the EHVL assumption I that the NE distribution function approaches the local equilibrium (LE) distribution function quickly compared with the rate of decay of the VACF. With this assumption the local tagged particle current density can be approximated by

$$\sum_{\mathbf{r}} \sum_i c_{ix} f_i^{\text{NE}}(\mathbf{r}, t) \approx \sum_{\mathbf{r}} P(\mathbf{r}, t) u_x(\mathbf{r}, t), \quad (6)$$

where

$$P(\mathbf{r}, t) = \sum_i f_i^{\text{NE}}(\mathbf{r}, t) \quad (7)$$

is the density of tagged particles in the NE ensemble, and

$$u_x(\mathbf{r}, t) = \frac{1}{\rho} \sum_i c_{ix} \langle s_i(\mathbf{r}, t) \rangle_{\text{NE}} \quad (8)$$

is the average fluid flow velocity, where ρ is the average number of particles per site in the equilibrium state. Introducing the Fourier transforms, we can write (6) as

$$\begin{aligned} \sum_{\mathbf{r}} \sum_i c_{ix} f_i^{\text{NE}}(\mathbf{r}, t) &= \frac{1}{V} \sum_{\mathbf{q} \in \text{1BZ}} u_{\mathbf{q}x}(t) P_{-\mathbf{q}}(t) \\ &\approx \int_{\mathbf{q} \in \text{1BZ}} d\mathbf{q} \frac{N_0}{(2\pi)^D} u_{\mathbf{q}x}(t) P_{-\mathbf{q}}(t). \end{aligned} \quad (9)$$

Here 1BZ denotes the first Brillouin zone of the reciprocal lattice corresponding to the lattice of cells. N_0 is the

number of lattice nodes per unit volume in the reciprocal space and D is the dimensionality of the system. For the FHP lattice and the FCHC lattice, N_0 is $\frac{1}{2}\sqrt{3}$ and 1, respectively. Note that the course graining has removed the largest \mathbf{q} modes from the summation. To determine the long-time behavior of (9) we use the solution of the diffusion equation for the tagged particle density,

$$P_{\mathbf{q}}(t) = e^{-D_0 q^2 t} P_{\mathbf{q}}(0), \quad (10)$$

and the hydrodynamic modes for $u_{\mathbf{q}x}(t)$, namely,

$$u_{\mathbf{q}x}(t) = \hat{q}_x u_{\mathbf{q}}^{\parallel}(t) + \hat{q}_x^{\perp} u_{\mathbf{q}}^{\perp}(t).$$

The first component decays as a sound mode. The second term decays as shear mode:

$$u_{\mathbf{q}}^{\perp}(t) = e^{-\nu_0 q^2 t} u_{\mathbf{q}}^{\perp}(0) = e^{-\nu_0 q^2 t} (\delta_{\alpha x} - \hat{q}_\alpha \hat{q}_x) u_{\mathbf{q}\alpha}(0). \quad (11)$$

Here D_0 is the “bare” or Boltzmann-Enskog diffusion coefficient, and ν_0 is the “bare” kinematic viscosity. The initial values of (7) and (8) are, with the use of (3), equal to $\delta_{\mathbf{r}\mathbf{r}_0}$ and $c_{i_0 x}(1 - \rho/b)\delta_{\mathbf{r}\mathbf{r}_0}$, respectively. Consequently the Fourier components at $t=0$ are

$$P_{\mathbf{q}}(0) = 1, \quad (12)$$

$$u_{\mathbf{q}\alpha}(0) = \frac{c_{i_0 \alpha}}{\rho} \left[1 - \frac{\rho}{b} \right], \quad (13)$$

$$u_{\mathbf{q}}^{\perp}(0) = \frac{c_{i_0 \alpha}}{\rho} (\delta_{\alpha x} - \hat{q}_\alpha \hat{q}_x) \left[1 - \frac{\rho}{b} \right]. \quad (14)$$

Insertion of (10)–(14) into (9) yields

$$\begin{aligned} \sum_{\mathbf{r}} \sum_i c_{ix} f_i^{\text{NE}}(\mathbf{r}, t) &= \int_{\mathbf{q} \in \text{BZ}_1} d\mathbf{q} \frac{N_0}{(2\pi)^D} e^{-(D_0 + \nu_0)q^2 t} \frac{c_{j_0 \alpha}}{\rho} \\ &\quad \times (\delta_{\alpha x} - \hat{q}_\alpha \hat{q}_x) \left[1 - \frac{\rho}{b} \right] \\ &\approx \frac{D-1}{D} \frac{c_{i_0 \alpha}(1 - \rho/b)N_0}{\rho[4\pi(D_0 + \nu_0)t]^{D/2}}. \end{aligned} \quad (15)$$

Inserting this expression into (5) yields

$$\begin{aligned} \langle v_x(0)v_x(t) \rangle &= \frac{D-1}{D} \frac{N_0(1 - \rho/b)\langle v_x^2(0) \rangle}{\rho[4\pi(D_0 + \nu_0)t]^{D/2}} \\ &= \frac{d_0^* \langle v_x^2(0) \rangle}{t^{D/2}} = \frac{d_0}{t^{D/2}}, \end{aligned} \quad (16)$$

where d_0^* is the normalized tail coefficient. Note that this expression differs by a factor $(1 - \rho/b)$ from the continuous expression. This factor is a consequence of the Fermi statistics and guarantees that the state occupied by the tagged particle contains no fluid particle. The values of the parameters b , $\langle v_x^2(0) \rangle$, and N_0 in formula (16) are, respectively, 7, $\frac{3}{2}$, and $\frac{1}{2}\sqrt{3}$ for the FHP-III model and 24, $\frac{1}{2}$, and 1 for the FCHC model.

IV. COMPUTATIONAL TECHNIQUE

In this section we discuss our new technique to calculate the VACF of a tagged particle in a simulation. We wish to stress that the present form of this method is only applicable to the calculation of the correlation function of one tagged particle and is not, for instance, suitable for calculating the stress correlation function.

In the techniques used thus far^{1,6,7} a single tagged particle is followed along its classical trajectory. An estimate of $\langle v_x(0)v_x(t) \rangle$ is then obtained as an average of $v_x(0)v_x(t)$ over different time origins in this trajectory, different particles, and different initial conditions. To obtain reasonable statistics with these “brute force” methods, one needs lengthy simulations on large systems. For discrete systems^{9,10} these methods could not be used to calculate the VACF in the region $t \gg t_0$ with enough accuracy to observe any algebraic tail at all.

We will now present a method, the moment-propagation (MP) method, that is about a million times more efficient and easily implemented on vector computers. The basic idea will be given in three steps.

First, let us consider one tagged particle, say a “blue” particle, in a lattice with other, but identical “red” particles. We now make use of the fact that in LGCA a particle loses its identity in a collision. So in a collision with a blue particle involved, it is not possible to tell which one of the postcollisional outgoing particles was the incoming blue particle. We now choose our stochastic collision rules such that any outgoing particle is equally likely to be the blue particle. So instead of one defined path of the particle, there are now a lot of possible paths, each associated with a certain probability. We can compute this probability as the product of the scattering probabilities. The average of $v_x(0)v_x(t)$ of the blue particle is the sum over all paths of $v_x(0)v_x(t)$, each path contribution weighted with the appropriate probability factor. Note that only $v_x(t)$ is “path dependent.”

Second, we do not need to know which specific path a particle has followed; as a matter of fact, we are only interested in the probability that the blue particle arrives at time t on site \mathbf{r} , because all the paths going to (\mathbf{r}, t) will result in the same $v_x(t)$. This site probability is clearly constructed as the sum of the probabilities of all paths ending at this site. This makes things much easier, for now we can just transport at every time step this probability to the neighbor sites multiplied by the probability that the tagged particle would go that way. Note that at $t=0$ the site probability for the “starting” site is equal to one, and for all the other sites equal to zero.

Finally, we now think of every particle in the lattice as a starting particle. We can just add the contribution of all particles to the site probability, under the condition that the initial site probability of the starting particles is weighted with their initial velocity $v_x(0)$. Note that this procedure corresponds to propagating the v_x velocity of the particles. The correlation function $\langle v_x(0)v_x(t) \rangle$ is now equal to the sum over all sites of this site probability at time t , multiplied by the average site velocity at that time, i.e., we propagated the first moment of the single-particle velocity distribution function. More generally,

we can propagate any moment of the single-particle distribution function.

The method is conveniently summarized by the following equations: Let us define the number of particles N as

$$N = \sum_{\mathbf{r}} \sum_i s_i(\mathbf{r}, 0)$$

and the average site velocity,

$$\bar{v}_x(\mathbf{r}, t) = \sum_i \left[\frac{s_i(\mathbf{r}, t)}{\sum_j s_j(\mathbf{r}, t)} c_{ix} \right].$$

The sum over all tagged particles of the probability to find one individual tagged particle at site \mathbf{r} weighted with its initial velocity is denoted by $W(\mathbf{r}, t)$, and evolves in time as

$$W(\mathbf{r}, t+1) = \sum_i \left[W(\mathbf{r}-\mathbf{c}_i, t) \frac{s_i(\mathbf{r}-\mathbf{c}_i, t)}{\sum_j s_j(\mathbf{r}-\mathbf{c}_i, t)} \right], \quad \forall \mathbf{r}$$

where the initial value $W(\mathbf{r}, 1)$ is given by

$$W(\mathbf{r}, 1) = \sum_i s_i(\mathbf{r}-\mathbf{c}_i, 0) c_{ix}.$$

The VACF at time t is now simply given by

$$\langle v_x(0)v_x(t) \rangle = \frac{1}{N} \sum_{\mathbf{r}} W(\mathbf{r}, t) \bar{v}_x(\mathbf{r}, t).$$

Note that the averaging is all possible paths of one tagged particle and in turn over all possible particles. At t time steps, the number of possible paths of one particle is of the order ρ^t , where ρ is the average number of particles per site. As a result, the averaging is over approximately $N\rho^t$ different events, although not totally uncorrelated. Nevertheless, this greatly improves the statistics, with the convenient effect that the accuracy increases with increasing t , which makes the method extremely useful for calculating the VACF for longer times. The only additional averaging is over different time origins, and over different initial conditions in order to estimate the statistical error. In our simulations using this new technique we observed statistical errors of the order of 10^{-6} in both two and three dimensions. Compared with the only known simulation results for two-dimensional LGCA using conventional techniques,^{9,10} this corresponds to a gain of 10^6 in computer time. This method allows us to calculate the VACF with enough accuracy in the region $t \gg t_0$ to serve as a serious test of mode-coupling theory, without making use of any other approximations than those within the LGCA framework.

V. SIMULATION

A. General aspects

The simulations were carried out on systems of up to 500×500 lattice points in two dimensions and $60 \times 60 \times 60$ lattice points in three dimensions. In all cases correlations were only computed for time intervals less than the shortest time in which any particle could

cross the periodic box. This in contrast to corresponding simulations of long-time tails in atomic fluids,^{6,7} where time intervals up to five times the acoustic wave traversal time had to be used. In the present simulation the VACF is calculated for different densities varying from $d=0.05$ to 0.90, where d is defined as the average number of particles per link per node ($d = \rho/b$). In order to estimate the statistical error of the VACF, five to ten independent simulations per density were performed. All calculations were performed on a NEC-SX2 supercomputer.

B. Results and discussion

We will give here the simulation results and compare them with the theory. All results shown are related to correlation functions normalized to one at $t=0$. The three-dimensional case will be discussed first and in most detail, whereas for two dimensions only the main result will be shown. For more details, see Ref. 20.

Figure 1 shows the VACF of a tagged particle in the 3D lattice at a density $d=0.10$. Both the simulation data and the theoretical prediction are shown, and as we see the agreement is quite good. Initially the decay is approximately exponential, and after about ten collision times the algebraic tail is clearly observed. We note that characteristic decay time t_0 of the exponential part is about 1.1 for this density. We also observe a decreasing statistical error with increasing time, as expected. Note that the error is of the order 10^{-6} .

For higher densities the statistics is even better as shown in Fig. 2, where we show the VACF for $d=0.75$ from simulations only. After about ten collision times the function decays as t^a with $a = -1.516 \pm 0.005$, which should be compared to the value $a = -\frac{3}{2}$ that is predicted

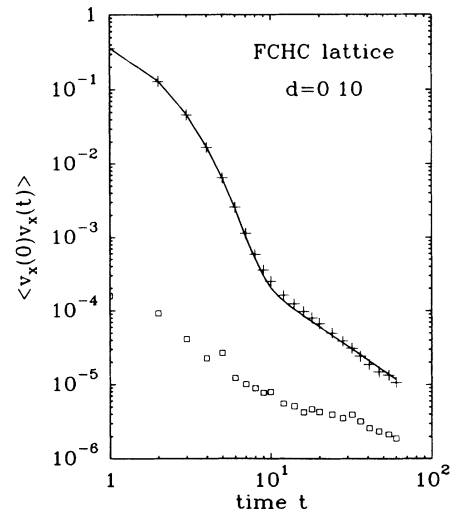


FIG. 1. Log-log plot of the normalized velocity autocorrelation function of a three-dimensional lattice-gas cellular automaton on a FCHC lattice for density $d=0.10$. The time is in units of the unit time step ΔT of the LGCA. The solid line is the prediction of mode-coupling theory; the crosses are the simulation data. Note that the estimated error (open squares) decreases with increasing t to a value of order 10^{-6} .

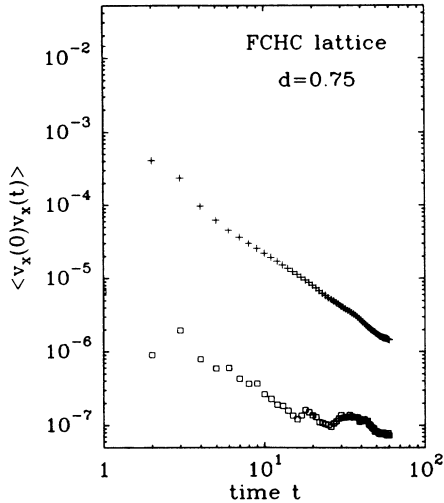


FIG. 2. As in Fig. 1, but for density $d=0.75$. Only the simulation data are shown. Note that after an initial rapid decay, the VACF approaches a power-law decay with an exponent -1.516 .

for hydrodynamic long-time tails. To our knowledge this is the most accurate verification of the exponent of the algebraic long-time tail of the VACF of a 3D fluid. A more convenient representation of the algebraic long-time tails is shown in Fig. 3, where we plotted the VACF multiplied by $t^{3/2}$, for different densities. We expect these functions to approach a constant value as $t \rightarrow \infty$. Such behavior is indeed observed. This in itself may not be surprising, but it is reassuring as it has been argued that the hydrodynamic long-time tails observed in computer simulations on continuous systems may be due to a propagation of numerical errors.²¹ In the present simula-

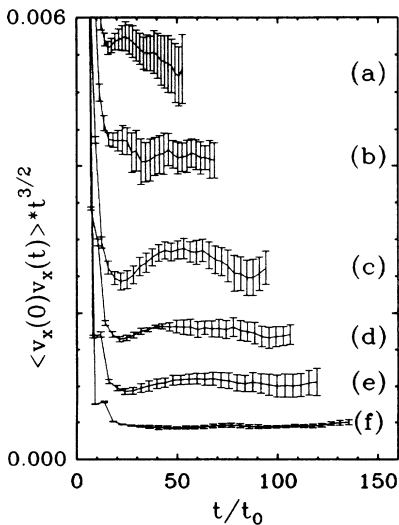


FIG. 3. Velocity autocorrelation function multiplied by $t^{3/2}$ for different densities: (a) $d=0.2$, (b) $d=0.3$, (c) $d=0.5$, (d) $d=0.6$, (e) $d=0.7$, (f) $d=0.8$. The time is in units of mean free time t_0 .

tion the discrete dynamics of the lattice gas is solved exactly; hence propagation of numerical errors is ruled out as a factor affecting the power-law tails.

Next we look at the tail coefficient d_0^* defined in formula (16), as a function of the density. In Fig. 4 both the prediction of mode-coupling theory and the simulation data are shown, where the latter are the plateau values of Fig. 3 supplied with the results for some other densities. As can be seen from Fig. 4, we find agreement between theory and simulation within the estimated statistical error. We wish to stress that the theoretical and simulation results were obtained completely independently and that we did not make use of any adjustable parameter. The comparison is shown more clearly in Fig. 5, where we plotted d_0^* divided by $d^{1/2}$, to divide out the leading non-analytic part in the density dependence of d_0^* in formula (13) as $d \rightarrow 0$. The dashed curve in Fig. 5 is a third-order polynomial fit to the simulation data. As we see, the agreement with the theoretical curve is almost perfect.

In two dimensions the results are qualitatively similar and details are published elsewhere.²⁰ For now we shall only present d_0^* as a function of d , both simulation results, and theory (see Fig. 6). As we see, mode-coupling theory overestimates the amplitude by at most 5% in two dimensions. This small deviation cannot be due to a trivial numerical factor because in the exponential regime the VACF agrees with the theory within the estimated error, which is only of the order of 0.1%. At present we have no explanation why the agreement between simulation and mode-coupling theory is worse in two dimensions than in three (where theory and simulations are essentially indistinguishable).

It might be argued that we should have used the true transport coefficients D and ν in Eq. (13), rather than the bare coefficients D_0 and ν_0 . In three dimensions the correction to the bare diffusion constant D_0 can be estimated by numerical integration of the VACF obtained in our simulations. This yields a value of D that is at most one percent larger than the Enskog value D_0 . Simi-

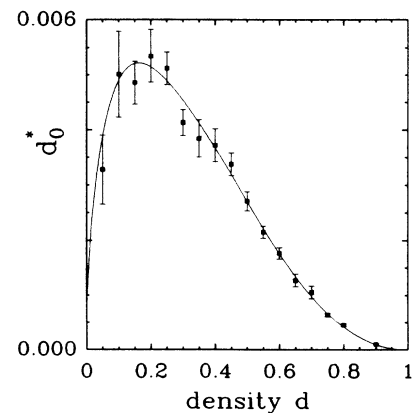


FIG. 4. Normalized tail coefficient d_0^* for the three-dimensional system as a function of the density [see Eq. (16)]. The solid line is the prediction of mode-coupling theory; the points are the simulation data. The density is in units of average number of particles per link.

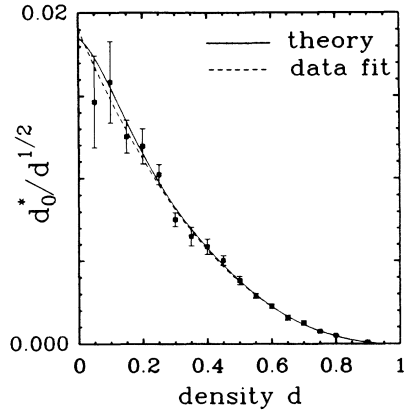


FIG. 5. The normalized tail coefficient for the 3D system divided by $d^{1/2}$. The solid curve is the theoretical curve; the dashed curve is a weighted fit to the simulation data.

larly, the difference between ν and ν_0 proved to be very small.²² Of course, in two dimensions the true transport coefficients D and ν diverge. Hence, we cannot make the same comparison in that case. However, an earlier study by Frenkel and Ernst²⁰ suggests that in the time regime studied in the present simulations, the corrections to the VACF due to the divergence of the transport coefficients themselves are still relatively small. Another factor that might influence the mode-coupling prediction is the presence of spurious invariants. It is known that many LGCA models have spurious “unphysical” conserved quantities that are related to the discrete nature of the model and may couple to the hydrodynamic modes.²³ However, none of the known invariants in either the FHP-III model or the FCHC model has the right symmetry to affect the results of the lowest-order mode-coupling theory [Eq. (16)].

In summary we have presented a new technique that allowed us to calculate the velocity autocorrelation function in a simulation with sufficient accuracy to give a quantitative estimate of the amplitude of the hydrodynamic long-time tail. In this way we could test the pre-

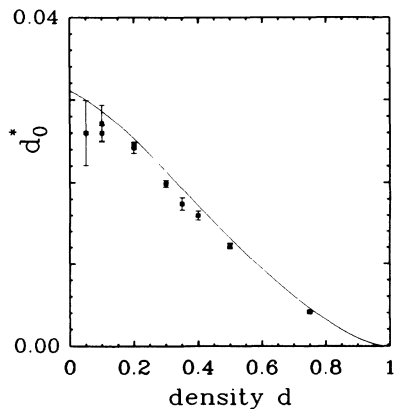


FIG. 6. Like Fig. 4, but for the two-dimensional system.

diction of mode-coupling theory for the density dependence of this amplitude. In two dimensions, such a comparison showed small deviations of up to 5% with the simulation results. In three dimensions the comparison indicated that, for all densities studied, the coefficient of the algebraic long-time tail is predicted by mode-coupling theory within the (small) statistical error. This finding strongly supports the validity of the basic assumptions of mode-coupling theory for 3D atomic fluids in general.

ACKNOWLEDGMENTS

The derivation of the mode-coupling theory for lattice gases given in Sec. III is due to M. H. Ernst, whom we thank for giving us permission to include this derivation in the present paper. We also thank Ernst for his interest in this work. We would like to thank Tony Ladd for stimulating discussions and the steady exchange of information. This work is part of the research program of the Stichting voor Fundamenteel Onderzoek der Materie (Foundation for Fundamental Research on Matter) and was made possible by financial support from the Nederlandse Organisatie voor Zuiver Wetenschappelijk Onderzoek (Netherlands Organization for the Advancement of Research). Computer time on the NEC-SX2 at Nationaal Lucht-en Ruimtevaartkundig Laboratorium was made available through a grant by the NFS (Nationaal Fonds Supercomputers).

APPENDIX A: VISCOSITY AND DIFFUSION COEFFICIENT OF THE THREE-DIMENSIONAL LGCA

In this appendix we give the explicit expressions for the kinematic viscosity ν_0 and the Enskog diffusion

TABLE I. Coefficients C_p and A_p determining, respectively, the kinematic viscosity and the Enskog diffusion coefficient. p is the number of particles.

p	C_p	A_p
1	0	1
2	4	11
3	78	77
4	718	385
5	4170	1463
6	17 296	4389
7	54 828	10 659
8	137 952	21 318
9	280 756	35 530
10	465 708	49 742
11	630 920	58 786
12	698 148	58 786
13	630 920	49 742
14	465 708	35 530
15	280 756	21 318
16	137 952	10 659
17	54 828	4389
18	17 296	1463
19	4170	385
20	718	77
21	78	11
22	4	1
23	0	0
24	0	0

coefficient D_0 from lattice-gas theory for the three-dimensional FCHC model used in the present paper.

Hénon²⁴ showed that in the Boltzmann approximation the kinematic viscosity in three dimensions is equal to

$$\nu_0 = \frac{c^2}{6} \left(\lambda - \frac{1}{2} \right), \quad (17)$$

where

$$\frac{1}{\lambda} = \frac{4}{3} \sum_{s,s'} \left[(s_i - s'_i) d^{p-1} (1-d)^{b-p-1} \times \sum_{j=1}^b s_j \cos^2 \theta_{ij} \right]. \quad (18)$$

Here $A(s, s')$ is the collision matrix, $p = \sum_{i=1}^b s_i$ is the number of particles of a one-node state s , d is the density in particles per link ($d = \rho/24$), and θ_{ij} is the angle between \mathbf{c}_i and \mathbf{c}_j . The summation $\sum_{s,s'}$ is over all possible input and output states. From (18) we can collect terms with the same number of particles p and write (17) and (18) in the form (with $c^2 = 2$ and $b = 24$)

$$\nu_0 = \frac{1}{4} \left[\sum_{p=1}^{24} C_p d^{p-1} (1-d)^{23-p} \right]^{-1} - \frac{1}{6}. \quad (19)$$

The coefficients C_p for the lattice-gas model studied in the present paper are given in Table I.

For time discrete systems the Enskog diffusion coefficient is given by

$$D_0 = \frac{1}{2} \langle v_x^2(0) \rangle + \sum_{n=1}^{\infty} \langle v_x(0) v_x(n) \rangle. \quad (20)$$

In the Enskog approximation this may be written as

$$\begin{aligned} D_0 &= \frac{1}{2} \langle v_x^2(0) \rangle + \langle v_x^2(0) \rangle \sum_{n=1}^{\infty} [Z_N(1)]^n \\ &= \frac{1}{2} \langle v_x^2(0) \rangle + \langle v_x^2(0) \rangle \frac{Z_N(1)}{1 - Z_N(1)}, \end{aligned} \quad (21)$$

with $Z_N(k)$ the normalized correlation function

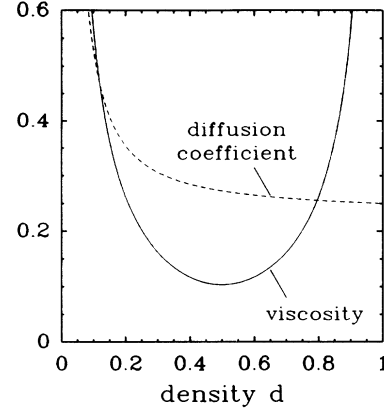


FIG. 7. Kinematic viscosity (solid line) and Enskog diffusion coefficient (dashed line) for the 3D model as calculated from the formulas (19), (21), and (22), and Table I.

$$Z_N(k) = \frac{\langle v_x(0) v_x(k) \rangle}{\langle v_x^2(0) \rangle}.$$

In lattice gases the correlation function after one time step is given by

$$Z_N(1) = \sum_s d^{p-1} (1-d)^{24-p} \sum_{i=1}^{24} \frac{s_i c_{ix}}{\sum_j s_j},$$

where the summation is over all configurations with $s_1 = 1$, with the convention that $c_{1x} = 1$. This again can be written as

$$Z_N(1) = \sum_{p=1}^{24} A_p d^{p-1} (1-d)^{24-p}, \quad (22)$$

where the coefficients A_p are given in Table I. The diffusion constant and the viscosity are both shown in Fig. 7, with $\langle v_x^2(0) \rangle = 0.5$.

- ¹B. J. Alder and T. E. Wainwright, *Phys. Rev. A* **1**, 18 (1970).
²J. R. Dorfman and E. G. D. Cohen, *Phys. Rev. Lett.* **25**, 1257 (1970); *Phys. Rev. A* **6**, 776 (1972); **12**, 292 (1975).
³M. H. Ernst, E. H. Hauge, and J. M. J. van Leeuwen, *Phys. Rev. A* **4**, 2055 (1971).
⁴Y. Pomeau and P. Resibois, *Phys. Rep.* **19**, 63 (1975).
⁵D. Levesque and W. T. Ashurst, *Phys. Rev. Lett.* **33**, 277 (1974).
⁶J. J. Erpenbeck and W. W. Wood, *Phys. Rev. A* **26**, 1648 (1982).
⁷J. J. Erpenbeck and W. W. Wood, *Phys. Rev. A* **32**, 412 (1985).
⁸U. Frisch, B. Hasslacher, and Y. Pomeau, *Phys. Rev. Lett.* **56**, 1505 (1986).
⁹J.-P. Boon and A. Noullez, in *Proceedings of the Workshop on Discrete Kinetic Theory, Lattice Gas Dynamics and Foundations of Hydrodynamics, Torino, Italy, 1988*, edited by R. Monaco (World Scientific, Singapore, 1989). Subsequent analyses by Boon and Noullez (1989) suggest that their simulation data are compatible with the presence of a long-time

- tail of approximately the correct amplitude.
¹⁰P. M. Binder and D. d'Humières, Los Alamos Report No. LA-UR-1341 1988 (unpublished) and in proceedings (see Ref. 9).
¹¹U. Frisch, D. d'Humières, B. Hasslacher, P. Lallemand, Y. Pomeau, and J.-P. Rivet, *Complex Systems* **1**, 649 (1987).
¹²D. d'Humières and P. Lallemand, *Complex Systems* **1**, 599 (1987).
¹³D. d'Humières, P. Lallemand, and U. Frisch, *Europhys. Lett.* **2**, 291 (1986).
¹⁴J.-P. Rivet, M. Hénon, U. Frisch, and D. d'Humières, *Europhys. Lett.* **7**, 231 (1988).
¹⁵A. J. C. Ladd and D. Frenkel, in *Proceedings of the Workshop on Cellular Automata and Modelling of Complex Physical Systems, Les Houches, 1989*, edited by P. Manneville (Springer, Berlin, 1989).
¹⁶M. Hénon, *Complex Systems* **1**, 475 (1987).
¹⁷J. A. Somers and P. C. Rem, in *Proceedings of the Workshop on Cellular Automata and Modelling of Complex Physical Sys-*

- tems*, edited by P. Manneville (Springer, Berlin, 1989).
- ¹⁸L. P. Kadanoff, G. McNamara, and G. Zanetti, *Phys. Rev. A* **40**, 4527 (1989).
- ¹⁹M. H. Ernst, in *Proceedings of the NATO Workshop on Lattice Gas Methods for PDE's, Los Alamos, 1989*, edited by G. Doolen [Physica D (to be published)].
- ²⁰D. Frenkel and M. H. Ernst, *Phys. Rev. Lett.* **63**, 2165 (1989).
- ²¹R. F. Fox, *Phys. Rev. A* **27**, 3216 (1983).
- ²²A. J. C. Ladd (private communication).
- ²³G. Zanetti, *Phys. Rev. A* **40**, 1539 (1989).
- ²⁴M. Hénon, *Complex Systems* **1**, 763 (1987).